Quasi-Static Image Method Applied to Bi-Isotropic Microstrip Geometry

Päivi K. Koivisto and Johan C.-E. Sten

Abstract—**A generalization of the partial image method, applicable for static planar-layered problems, is used to form Green's functions for the layered structure involving bi-isotropic medium. The results are applied for the analysis of a microstrip transmission line assumed to support the quasi-TEM mode. The capacitance and inductance per unit length are calculated to determine the propagation factor and impedance for the structure composed of a conducting strip attached to a bi-isotropic slab with conducting backing.**

Index Terms—**Bi-isotropic medium, image method, quasi-static approximation.**

I. Introduction

Bi-ISOTROPIC (BI) medium has attracted a growing interest in recent years because of the extra medium parameters, which offer a better possibility to modify different structures that usually contain only dielectric or magnetic media. The BI medium can be characterized by four scalar medium parameters ϵ, μ, ξ, and ζ, relating the quantities of the electromagnetic field through the following type of constitutive relations:

$$\mathbf{D} = \epsilon\mathbf{E} + \xi\mathbf{H} \qquad \mathbf{B} = \mu\mathbf{H} + \zeta\mathbf{E} \tag{1}$$

where

$$\xi = (\chi - j\kappa)\sqrt{\epsilon_0\mu_0} \qquad \zeta = (\chi + j\kappa)\sqrt{\epsilon_0\mu_0} \tag{2}$$

The permittivity ω, permeability μ are assumed independent of frequency, whereas the chirality κ is inherently connected with Ω and its effect vanishes at zero frequency. The additional parameter χ describes the magneto-electric effect, which causes nonreciprocity of the medium.

In the present article, the method of partial images introduced by Silvester [1], is generalized for BI media and applied to find Green's functions for point and line sources in BI microstrip geometry. The static image method for BI media was introduced by Lindell for plane parallel interfaces [2] and followed by a generalization for cylindrical interfaces [3]. The same author has also developed an image theory for the bi-isotropic sphere [4].

The microstrip is a popular form of inhomogeneous two-conductor transmission line used in many of today's microwave applications. The theory of quasi-TEM modes in multidielectric microstrip structure was originally discussed by dos Santos and Figanier [5] and generalized for multiconductor lines by Lindell [6]. The method is based on the expansion of the propagation factor as well as the field components in power series of Ω. The quasi-TEM mode consists of combinations of electrostatic and magnetostatic fields, related by their boundary values, and longitudinal field components that arise from the transverse fields. In this article, the quasi-static solution of the microstrip is analyzed when the substrate medium is assumed bi-isotropic. The capacitance and the inductance of the structure per unit length are computed to obtain the propagation factor and characteristic impedance. The influence of the parameter χ on the propagation factor, phase velocity, and impedance are represented graphically for different permittivities.

Manuscript received February 23, 1993; revised March 4, 1994. This work was supported by the Academy of Finland.

The authors are with the Electromagnetics Laboratory at the Helsinki University of Technology, FIN-02150 Espoo, Finland.

IEEE Log Number 9406797.

II. Theory

A. Electrostatic Fields

Consider the problem of an electric and magnetic point charge, q_e and q_m with the same location $\mathbf{r}'$. The fields which the charges develop satisfy the static Maxwell equations, written in the operational form

$$\nabla \times \mathbf{e} = \mathbf{0} \qquad \nabla \cdot \mathbf{d} = \mathcal{Q}\delta(\mathbf{r} - \mathbf{r}') \tag{3}$$

and the medium equations for the general BI medium

$$\mathbf{d} = \mathcal{M}\mathbf{e} \tag{4}$$

where the field and source quantities are represented by the matrices

$$\mathbf{e} = \begin{pmatrix} \mathbf{E} \\ \mathbf{H} \end{pmatrix} \quad \mathbf{d} = \begin{pmatrix} \mathbf{D} \\ \mathbf{B} \end{pmatrix} \quad \mathcal{Q} = \begin{pmatrix} q_e \\ q_m \end{pmatrix} \tag{5}$$

and the medium matrix $\mathcal{M}$ by

$$\mathcal{M} = \begin{pmatrix} \epsilon & \xi \\ \zeta & \mu \end{pmatrix} \tag{6}$$

Because the field matrix $\mathbf{e}$ is irrotational, we are free to introduce the potential matrix

$$\Phi = \begin{pmatrix} \phi_e \\ \phi_m \end{pmatrix} \tag{7}$$

satisfying $\mathbf{e} = -\nabla\Phi$ and, because of (3) and (4), the Poisson equation

$$\mathcal{M}\nabla^2\Phi = -\mathcal{Q}\delta(\mathbf{r} - \mathbf{r}') \tag{8}$$

where ϕ_e is the electric and ϕ_m the magnetic scalar potential. The solution to (8) is of the form

$$\Phi = \frac{1}{4\pi D}\mathcal{M}^{-1}\mathcal{Q} \tag{9}$$

with D being the distance between the source point $\mathbf{r}'$ and the observation point $\mathbf{r}$. Thus, the potentials due to an electric point charge q_e in BI medium can be written

$$\phi_e = \frac{q_e}{4\pi(\epsilon - \xi\zeta/\mu)D} \qquad \phi_m = \frac{-\zeta}{\mu}\phi_e \tag{10}$$

Let the point charge $\mathcal{Q}$ be located at $z' > 0$ in medium $\mathcal{M}_1$ in front of a half space $z < 0$ of medium $\mathcal{M}_2$. The reflection and transmission images can be solved from two boundary conditions [2]. Let the transmission and reflection images be point charges $\mathcal{Q}_t$ and $\mathcal{Q}_r$ at the original source point $z = z'$ and at the mirror image point $z = -z'$, respectively. The incident, transmitted, and reflected potentials are

$$\Phi_i = \frac{\mathcal{M}_1^{-1}\mathcal{Q}}{4\pi D} \qquad \Phi_t = \frac{\mathcal{M}_2^{-1}\mathcal{Q}_t}{4\pi D_t} \qquad \Phi_r = \frac{\mathcal{M}_1^{-1}\mathcal{Q}_r}{4\pi D_r} \tag{11}$$

with the distance functions

$$D = D_t = \sqrt{\rho^2 + (z - z')^2} \quad D_r = \sqrt{\rho^2 + (z + z')^2} \tag{12}$$

Continuity of the potential and the normal component of the displacement vector $\mathbf{d}$ at $z = 0$ gives the equation pair

$$\mathcal{M}_1^{-1}\mathcal{Q} + \mathcal{M}_1^{-1}\mathcal{Q}_r = \mathcal{M}_2^{-1}\mathcal{Q}_t \tag{13}$$

$$\mathcal{Q} - \mathcal{Q}_r = \mathcal{Q}_t \tag{14}$$

from which the image sources

$$\mathcal{Q}_t = \mathcal{M}_2 T \mathcal{M}_1^{-1}\mathcal{Q} \tag{15}$$

$$\mathcal{Q}_r = \mathcal{M}_1 R \mathcal{M}_1^{-1}\mathcal{Q} \tag{16}$$

can be solved. Here, T and R denote the transmission and reflection matrices respectively, which are

$$R = (\mathcal{M}_1 + \mathcal{M}_2)^{-1}(\mathcal{M}_1 - \mathcal{M}_2) = -I + T \tag{17}$$

$$T = 2(\mathcal{M}_1 + \mathcal{M}_2)^{-1}\mathcal{M}_1 \tag{18}$$

It is remarkable that even if the original source would be only an electric point charge, the images consist of both an electric and a magnetic point charges, provided that at least one of the medium matrices $\mathcal{M}_1$, $\mathcal{M}_2$ is nondiagonal (i.e. BI medium).

B. Magnetostatic Fields

Let us study the fields arising from static currents when free charges are absent. Then the Maxwell equations read

$$\nabla \times \mathbf{e} = \begin{pmatrix} -J_m \\ J_e \end{pmatrix}\delta(\mathbf{r} - \mathbf{r}') = \mathcal{J}\delta(\mathbf{r} - \mathbf{r}') \qquad \nabla \cdot \mathbf{d} = 0 \tag{19}$$

where $\mathbf{J}_e$ and $\mathbf{J}_m$ are electric and magnetic currents. Expressing the displacement vector matrix $\mathbf{d}$ by means of the magnetic vector potential matrix $\mathbf{a}$:

$$\mathbf{d} = \nabla \times \mathbf{a} = \nabla \times \begin{pmatrix} \mathbf{A}_e \\ \mathbf{A}_m \end{pmatrix} \tag{20}$$

and demanding that $\nabla \cdot \mathbf{a} = 0$, gives us the Poisson equation

$$\nabla^2 \mathbf{a} = -\mathcal{M}\mathcal{J}\delta(\mathbf{r} - \mathbf{r}') \tag{21}$$

which, when $\mathcal{M}$ is replaced by $\mathcal{M}^{-1}$, is similar to (8). It turns out that the electrostatic and magnetostatic solutions, including boundary conditions and image expressions, are formally similar except for the replacement $\mathcal{M} \leftrightarrow \mathcal{M}^{-1}$ and $\mathcal{Q} \rightarrow \mathcal{J}$ everywhere. Obviously, since $\mathbf{a}$ is divergenceless, the similarity applies only for two dimensional problems, e.g., for straight line sources.

C. Green's Functions for the Layered Geometry

Let us assume that the point source $\mathcal{Q}$ lies in medium $\mathcal{M}_1$ (see Fig. 1) above the BI slab of medium $\mathcal{M}_2$ backed with a medium $\mathcal{M}_3$. The medium matrices can be written

$$\mathcal{M}_1 = \begin{pmatrix} \epsilon_0 & 0 \\ 0 & \mu_0 \end{pmatrix} \quad \mathcal{M}_2 = \begin{pmatrix} \epsilon & \xi \\ \zeta & \mu \end{pmatrix} \quad \mathcal{M}_3 = \begin{pmatrix} \epsilon_3 & 0 \\ 0 & \mu_3 \end{pmatrix} \tag{22}$$

From (17) the reflection matrices (15) for the electrostatic potentials become

$$\begin{aligned} R_{23} &= (\mathcal{M}_2 + \mathcal{M}_3)^{-1}(\mathcal{M}_2 - \mathcal{M}_3) \\ &= \frac{1}{(\epsilon_3 + \epsilon)(\mu_3 + \mu) - \xi\zeta} \\ &\quad \times \begin{pmatrix} (\epsilon - \epsilon_3)(\mu + \mu_3) - \xi\zeta & 2\mu_3\xi \\ 2\epsilon_3\zeta & (\epsilon + \epsilon_3)(\mu - \mu_3) - \xi\zeta \end{pmatrix} \end{aligned} \tag{23}$$

$$\begin{aligned} R_{12} &= (\mathcal{M}_1 + \mathcal{M}_2)^{-1}(\mathcal{M}_1 - \mathcal{M}_2) = -R_{21} \\ &= \frac{1}{(\epsilon_0 + \epsilon)(\mu_0 + \mu) - \xi\zeta} \\ &\quad \times \begin{pmatrix} (\epsilon_0 - \epsilon)(\mu_0 + \mu) + \xi\zeta & -2\mu_0\xi \\ -2\epsilon_0\zeta & (\epsilon_0 + \epsilon)(\mu_0 - \mu) + \xi\zeta \end{pmatrix} \end{aligned} \tag{24}$$

From (18), the transmission matrices (16) are correspondingly

$$\begin{aligned} T_{12} &= 2(\mathcal{M}_1 + \mathcal{M}_2)^{-1}\mathcal{M}_1 \\ &= \frac{2}{(\epsilon_0 + \epsilon)(\mu_0 + \mu) - \xi\zeta}\begin{pmatrix} \epsilon_0(\mu_0 + \mu) & -\mu_0\xi \\ -\epsilon_0\zeta & \mu_0(\epsilon_0 + \epsilon) \end{pmatrix} \end{aligned} \tag{25}$$

$$T_{21} = 2(\mathcal{M}_1 + \mathcal{M}_2)^{-1}\mathcal{M}_2 = 2I - T_{12} \tag{26}$$

$$T_{23} = 2(\mathcal{M}_2 + \mathcal{M}_3)^{-1}\mathcal{M}_2 = I + R_{23} \tag{27}$$

In the limit $\epsilon_3 \rightarrow \infty$, $\mu_3 \rightarrow 0$, corresponding to a PEC (perfect electric conductor) backing, the matrices simplify into

$$R_{23} \rightarrow \begin{pmatrix} -1 & 0 \\ 2\zeta/\mu & 1 \end{pmatrix} \qquad T_{23} \rightarrow \begin{pmatrix} 0 & 0 \\ 2\zeta/\mu & 2 \end{pmatrix} \tag{28}$$

When $\mathcal{M}_3 = \mathcal{M}_1$, corresponding to air backing, $R_{23} = R_{21}$ and $T_{23} = T_{21}$.

The reflection and transmission matrices in (23)–(27) are calculated for single reflection and transmission at the interfaces. In order to get the total potentials at different regions of the microstrip structure, the method of partial images given by Silvester [1] and O'Neill [5] must be generalized for BI medium interfaces. The locations of the image points remain

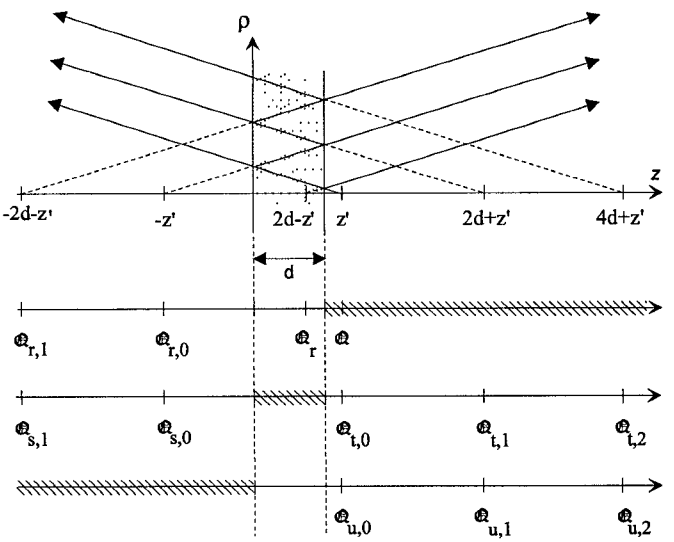

Fig. 1. Construction of multiple images due to a point charge $\mathcal{Q}$ (electric and magnetic point charge at the same location) in a layered structure. The arrows in the figure on the top represent flux lines. Location of images for the three regions are represented below.

the same as for isotropic media, but the scalar reflection and transmission coefficients must be replaced by the matrices (23)–(27).

Let us examine the problem represented in Fig. 1, where the thickness of the slab is d, and, taking the lower interface as the xy-plane, the location of the source is $z' > d$. For the potential in the upper medium $z > d$, we can write the amplitudes and the locations for the original and image point charges as 2

$$\begin{aligned} &\mathcal{Q} && z' \\ &\mathcal{Q}_r = \mathcal{M}_1 R_{12} \mathcal{M}_1^{-1} \mathcal{Q} && 2d - z' \\ &\mathcal{Q}_{r,0} = \mathcal{M}_1 T_{21} R_{23} T_{12} \mathcal{M}_1^{-1} \mathcal{Q} && -z' \\ &\quad \vdots \\ &\mathcal{Q}_{r,n} = \mathcal{M}_1 T_{21} (R_{23} R_{21})^n R_{23} T_{12} \mathcal{M}_1^{-1} \mathcal{Q} && -2nd - z \end{aligned} \tag{29}$$

Correspondingly, the potential in the BI layer can be obtained from image point charges in half space $z > d$

$$\begin{aligned} &\mathcal{Q}_{t,0} = \mathcal{M}_2 T_{12} \mathcal{M}_1^{-1} \mathcal{Q} && z' \\ &\quad \vdots \\ &\mathcal{Q}_{t,n} = \mathcal{M}_2 (R_{21} R_{23})^n T_{12} \mathcal{M}_1^{-1} \mathcal{Q} && 2nd + z' \end{aligned} \tag{30}$$

and image point charges in $z < 0$

$$\begin{aligned} &\mathcal{Q}_{s,0} = \mathcal{M}_2 R_{23} T_{12} \mathcal{M}_1^{-1} \mathcal{Q} && -z' \\ &\quad \vdots \\ &\mathcal{Q}_{s,n} = \mathcal{M}_2 (R_{23} R_{21})^n R_{23} T_{12} \mathcal{M}_1^{-1} \mathcal{Q} && -2nd - z' \end{aligned} \tag{31}$$

Image point charges for the potential valid in the region $z < 0$ are

$$\begin{aligned} &\mathcal{Q}_{u,0} = \mathcal{M}_3 T_{23} T_{12} \mathcal{M}_1^{-1} \mathcal{Q} && z' \\ &\quad \vdots \\ &\mathcal{Q}_{u,n} = \mathcal{M}_3 T_{23} (R_{21} R_{23})^n T_{12} \mathcal{M}_1^{-1} \mathcal{Q} && 2nd + z' \end{aligned} \tag{32}$$

Applying the present partial image solution for the point charge $\mathcal{Q}$ located above the slab, the electrostatic potentials in all areas can be written by just summing the solutions for the image point charges given in (29)–(32).

To be confident on the image solution, let us examine expressions for the potential due to a point source located at the upper interface, i.e. $z' \to d$. The complete set of potentials in regions $z > d$, $0 < z < d$, and $z < 0$ become

$$\Phi_1 = \frac{1}{4\pi} \left[\frac{I}{D} + T_{21} \sum_{n=0}^{\infty} \frac{R_{23}}{D_n} (R_{21} R_{23})^n \right] T_{12} \mathcal{M}_1^{-1} \mathcal{Q} \tag{33}$$

$$\Phi_2 = \frac{1}{4\pi} \left[\sum_{n=0}^{\infty} \left(\frac{I}{D_{t,n}} + \frac{R_{23}}{D_n} \right) (R_{21} R_{23})^n \right] T_{12} \mathcal{M}_1^{-1} \mathcal{Q} \tag{34}$$

$$\Phi_3 = \frac{1}{4\pi} T_{23} \left[\sum_{n=0}^{\infty} \frac{1}{D_{t,n}} (R_{21} R_{23})^n \right] T_{12} \mathcal{M}_1^{-1} \mathcal{Q} \tag{35}$$

respectively, where

$$D = \sqrt{\rho^2 + (z-d)^2} \quad D_n = \sqrt{\rho^2 + (z + (2n+1)d)^2}$$
$$D_{t,n} = \sqrt{\rho^2 + (z - (2n+1)d)^2}$$

Fig. 2 show an example of the potential curves corresponding to an electric unit point charge located on the surface of a BI slab of thickness d. These figures show clearly that the potentials are continuous on the interfaces $z = 0$ and $z = d$, which is also easily seen from expressions (33)–(35), where $D_{t,n} = D_n$ at $z = 0$, and $D_{t,n} = D_{n-1}$ and $D_{t,0} = D$ at $z = d$. Also the continuity of the normal components of $\mathbf{d}$ at both interfaces can be confirmed.

The electrostatic potential due to any charge distribution can be expressed as

$$\Phi(\mathbf{r}) = \int_V G(\mathbf{r}, \mathbf{r}') \mathcal{M}_1^{-1} \mathcal{Q}(\mathbf{r}') dV' \tag{36}$$

where V is the volume containing the source and $G(\mathbf{r}, \mathbf{r}')$ is the Green's function, satisfying

$$\nabla^2 G(\mathbf{r}, \mathbf{r}') = -I\delta(\mathbf{r} - \mathbf{r}') \tag{37}$$

Comparing with expression (8), the solution for the potential due to a point charge can be expressed as $\Phi = G(\mathbf{r}, \mathbf{r}') \mathcal{M}_1^{-1} \mathcal{Q}$. Thus, Green's functions are easily obtainable from the solution for the potentials.

For $z > d$ we have

$$\begin{aligned} G_1(\mathbf{r}, \mathbf{r}') = &\frac{I}{4\pi \sqrt{(\rho - \rho')^2 + (z - z')^2}} \\ &+ \frac{R_{12}}{4\pi \sqrt{(\rho - \rho')^2 + (z + z' - 2d)^2}} \\ &+ \sum_{n=0}^{\infty} \frac{T_{21} R_{23} (R_{21} R_{23})^n T_{12}}{4\pi \sqrt{(\rho - \rho')^2 + (z + z' + 2nd)^2}} \end{aligned} \tag{38}$$

For $0 < z < d$

$$\begin{aligned} G_2(\mathbf{r}, \mathbf{r}') = \frac{1}{4\pi} \sum_{n=0}^{\infty} \Bigg[&\frac{(R_{21} R_{23})^n T_{12}}{\sqrt{(\rho - \rho')^2 + (z - z' - 2nd)^2}} \\ &+ \frac{(R_{23} R_{23})^n T_{12}}{\sqrt{(\rho - \rho')^2 + (z + z' + 2nd)^2}} \Bigg] \end{aligned} \tag{39}$$

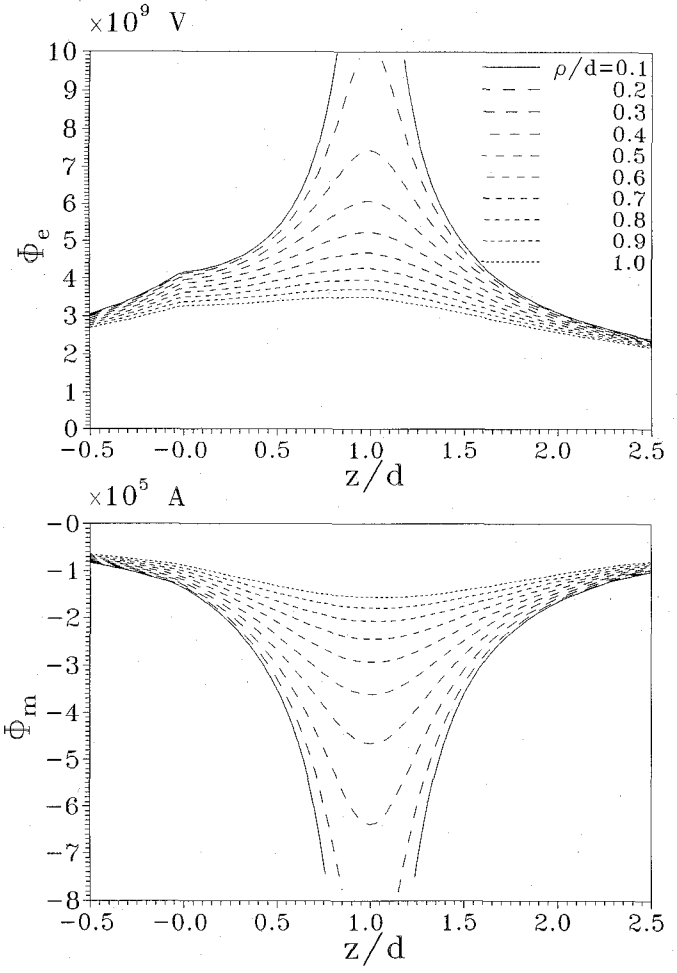

Fig. 2. The electric potential ϕ_e and magnetic potential ϕ_m corresponding to an electric unit point charge (1 As) on the surface of a BI slab with medium parameters $E_r = 10$, $M_r = 1$, $\chi = 0.1$, $K = 0$, located between $0 \leq z/d \leq 1$. The medium on both sides of the slab is air. The curves are drawn with different transverse distance ρ.

and for the lower half space $z < 0$

$$G_3(\mathbf{r}, \mathbf{r}') = \sum_{n=0}^{\infty} \frac{T_{23}(R_{21}R_{23})^n T_{12}}{4\pi\sqrt{(\rho-\rho')^2 + (z-z'-2nd)^2}} \tag{40}$$

All the above Green's functions are 2×2 matrices—the upper row for the electric potential and the lower for the magnetic potential.

D. Electric Line Sources

The electrostatic potential arising from a uniform infinite line charge along the y axis can be obtained by integrating the Green's functions (38)–(40) and choosing a convenient integration constant k. In fact, every inverse distance function can be replaced by a logarithm function in the following manner:

$$\frac{1}{\sqrt{(\rho-\rho')^2 + (z-z')^2}} \to -\ln[k^2((x-x')^2 + (z-z')^2)]$$

It can be shown that the Green's function for the magnetostatic problem, involving a straight line current $\mathcal{J}$, is very similar to (38)–(40) in the case of a line charge. The vector potential matrix $\mathbf{a}$, which is parallel to the current $\mathcal{J}$, can be expressed as

$$\mathbf{a}(\mathbf{r}) = \int_V G'(\mathbf{r}, \mathbf{r}') \mathcal{M}_1 \mathcal{J}(\mathbf{r}') dV' \tag{41}$$

where the Green's function G' is the same as (38)–(40) (written for a line charge). In this case, however, the reflection and transmission matrices are

$$R_{ij} = (\mathcal{M}_i^{-1} + \mathcal{M}_j^{-1})^{-1}(\mathcal{M}_i^{-1} - \mathcal{M}_j^{-1})$$
$$T_{ij} = 2(\mathcal{M}_i^{-1} + \mathcal{M}_j^{-1})^{-1}\mathcal{M}_i^{-1}$$

by virtue of (21).

III. Quasi-Static Solution for BI Microstrip

A. Quasi-TEM Fields

The quasi-static approximation is based on an asymptotic series expansion of the field quantities in terms of ω. The quasi-TEM fields in transversely inhomogeneous transmission lines are expressed as, [6]:

$$\mathbf{e}(\rho, y) = [\mathbf{e}_0(x,z) + j\omega\mathbf{e}_1(x,z) + \cdots]e^{-j\beta y}$$
$$\mathbf{d}(\rho, y) = [\mathbf{d}_0(x,z) + j\omega\mathbf{d}_1(x,z) + \cdots]e^{-j\beta y} \tag{42}$$

assuming that the field propagates in the y direction. The propagation factor is also written in a series form, beginning with $\beta = \omega\beta_1$.

Insertion of (42) in the Maxwell equations gives us the following set of zeroth-order equations:

$$\nabla \times \mathbf{e}_0 = \begin{pmatrix} 0 \\ \mathbf{J}_e \end{pmatrix} \qquad \nabla \cdot \mathbf{d}_0 = \begin{pmatrix} \varrho \\ 0 \end{pmatrix} \tag{43}$$

where the static electric current flows along the line $\mathbf{J}_e = \mathbf{u}_y I$ and ϱ is the charge induced on the conductor surfaces.

Since the chirality parameter is of first-order $\kappa = \omega\kappa_1$, it does not affect $\mathbf{d}_0$. Equation (43) shows that $\mathbf{e}_0$ and $\mathbf{d}_0$ are combinations of the electrostatic and magnetostatic two-dimensional field solutions, which can be expressed by the potentials as

$$\mathbf{E}_0 = -\nabla\phi_0$$
$$\mathbf{H}_0 = \frac{1}{\mu}\nabla A_0 \times \mathbf{u}_y + \frac{\chi\sqrt{\epsilon_0\mu_0}}{\mu}\nabla\phi_0$$
$$\mathbf{D}_0 = \frac{\chi\sqrt{\epsilon_0\mu_0}}{\mu}\nabla A_0 \times \mathbf{u}_y - \left(\epsilon - \frac{\chi^2\epsilon_0\mu_0}{\mu}\right)\nabla\phi_0$$
$$\mathbf{B}_0 = \nabla A_0 \times \mathbf{u}_y \tag{44}$$

where A_0 is the scalar part of the magnetic vector potential. The boundary conditions on the conductors

$$\mathbf{u}_n \times \mathbf{E}_0 = -\mathbf{u}_z \times \nabla\phi_0 = \mathbf{u}_y \frac{\partial}{\partial x}\phi_0 = 0$$
$$\mathbf{u}_n \cdot \mathbf{B} = \mathbf{u}_z \cdot (\nabla A_0 \times \mathbf{u}_y) = \frac{\partial}{\partial x}A_0 = 0 \tag{45}$$

implies that ϕ and A_0 are constant on both surfaces. Using these conditions and the formulas (36) and (41), the charge and current distributions in a given geometry can be computed.

The corresponding set of first-order equations can be written

$$\mu\mathbf{H}_0 + \nabla \times \mathbf{E}_1 = \beta_1 \mathbf{u}_y \times \mathbf{E}_0 - \chi\sqrt{\epsilon_0\mu_0}\,\mathbf{E}_0 \quad (46)$$

$$-\epsilon\mathbf{E}_0\nabla \times \mathbf{H}_1 = \beta_1 \mathbf{u}_y \times \mathbf{H}_0 + \chi\sqrt{\epsilon_0\mu_0}\,\mathbf{H}_0 \quad (47)$$

$$\epsilon\nabla \cdot \mathbf{E}_1 + \chi\sqrt{\epsilon_0\mu_0}\nabla \cdot \mathbf{H}_1 = \kappa_1\sqrt{\epsilon_0\mu_0}\nabla \cdot \mathbf{H}_0 \quad (48)$$

$$\mu\nabla \cdot \mathbf{H}_1 + \chi\sqrt{\epsilon_0\mu_0}\nabla \cdot \mathbf{E}_1 = -\kappa_1\sqrt{\epsilon_0\mu_0}\nabla \cdot \mathbf{E}_0 \quad (49)$$

The longitudinal components of the first order fields can be determined from the curl equations, and the transversal components from the divergence equations. In fact, inserting the fields (44) in (44)–(46) yields

$$\nabla \times \mathbf{E}_1 = \nabla \times [\mathbf{u}_y(\beta_1\phi_0 - A_0)] \quad (50)$$

$$\nabla \times \mathbf{H}_1 = -\nabla\left[\left(\epsilon - \frac{\chi^2\mu_0\epsilon_0}{\mu}\right)\phi_0 - \frac{\beta_1}{\mu}A_0\right] + \frac{\chi\sqrt{\mu_0\epsilon_0}}{\mu}\mathbf{u}_y \times \nabla(\beta_1\phi_0 - A_0) \quad (51)$$

$$\nabla \cdot \mathbf{H}_1 = \kappa_1\frac{\sqrt{\epsilon_0\mu_0}}{\mu}\nabla^2\phi_0 \qquad \nabla \cdot \mathbf{E}_1 = 0 \quad (52)$$

from where the solutions

$$\mathbf{E}_1 = \mathbf{u}_y(\beta_1\phi_0 - A_0) \quad (53)$$

$$\mathbf{H}_1 = \kappa_1\frac{\sqrt{\epsilon_0\mu_0}}{\mu}\nabla\phi_0 - \frac{\chi\sqrt{\epsilon_0\mu_0}}{\mu}\mathbf{u}_y(\beta_1\phi_0 - A_0) + \mathbf{u}_y H_1' \quad (54)$$

can be found. Here, the field H_1' is not known explicitly, but because it satisfies the equation

$$\nabla H_1' = -\mathbf{u}_y \times \nabla\left[\left(\epsilon - \frac{\chi^2\epsilon_0\mu_0}{\mu}\right)\phi_0 - \frac{\beta_1}{\mu}A_0\right] \quad (55)$$

its values can be calculated numerically. Equation (54) shows that the chirality gives rise to a transversal component for $\mathbf{H}_1$, which does not occur in the nonchiral case.

B. Circuit Quantities

To match the boundary condition $\mathbf{u}_n \times \mathbf{E} = \mathbf{u}_n \times \mathbf{E}_0 + j\omega\mathbf{u}_n \times \mathbf{E}_1 \cdots = 0$ on conducting surfaces, the equation

$$\beta_1\phi_0 - A_0 = 0 \quad (56)$$

for the y component of $\mathbf{E}_1$ (53) must be valid at both conductors. This condition yields

$$\beta_1 = \frac{A_a - A_b}{\phi_a - \phi_b} = \frac{\Psi_{ab}}{U_{ab}} \quad (57)$$

where U_{ab} and Ψ_{ab}, respectively, are the voltage and the magnetic flux between conductor a and b.

The divergence of (47) makes the left hand side vanish and integrating a unit length of the volume including the sources gives

$$\beta_1\int_V \nabla \cdot (\mathbf{u}_y \times \mathbf{H}_0)dV = -\int_V \nabla \cdot \mathbf{D}_0 dV \quad (58)$$

$$\Leftrightarrow \quad \beta_1\int_V \mathbf{J}_e(\mathbf{r})dV = \int_V \varrho(\mathbf{r})dV$$

from which a second relation

$$\beta_1 = \frac{Q_a}{I_a} \quad (59)$$

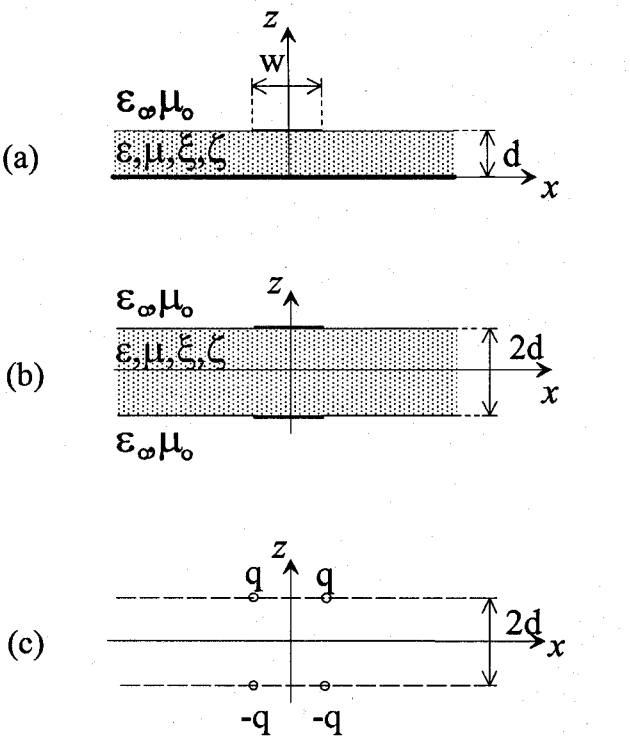

Fig. 3. (a) Cross-section of the original microstrip line. (b) Electrostatically equivalent line. (c) Model to form the Green's function.

can be obtained. Defining the capacitance C and the inductance L of the structure

$$\Psi_{ab} = LI_a \qquad Q_a = CU_{ab} \quad (60)$$

and using (57) and (59), the propagation constant β_1 can be expressed as

$$\beta_1 = \sqrt{\frac{\Psi_{ab}Q_a}{U_{ab}I_a}} = \sqrt{LC} \quad (61)$$

and the characteristic impedance as

$$Z = \frac{U_{ab}}{I_a} = \sqrt{\frac{L}{C}} \quad (62)$$

IV. Numerical Examples

The capacitance per unit length of the microstrip structure is determined using a finite element solution method [1]. An infinitely thin surface conductor of width w, extending from $y = -\infty$ to ∞, lies on the plane $z = d$ carrying a unit voltage, whence the $z = 0$ plane is taken as zero voltage, Fig. 3(a). The conductor is bounded by $x = \pm w/2$ and separated from the PEC plane by a substrate of thickness d. One of the problems is to solve for the electric charge density distribution induced on the conductor surface.

Since the surface charge distribution is longitudinally uniform, it can be modeled by $2N$ line conductors along the y direction in the $z = d$ plane, each carrying a constant charge density per unit length. Because the voltage of one strip is determined not only by the prescribed charge, but also by the charge that is induced by the other strips including itself, the formulation of the problem yields an integral equation. The

Green's function can be developed in a similar manner as was originally done by Silvester [1] for microstrips with dielectric substrates. As indicated in Fig. 3, the following geometric symmetry properties are exploited:

- The charge is symmetrically distributed in x-direction with respect to the y-axis.
- The original microstrip structure is replaced by an electrostatically equivalent structure, consisting of two conductor strips separated by the substrate slab of thickness $2d$ (Fig. 3(b)).
- Only the potential at the interface $z = d$ is of interest.

After some algebra, we obtain the expression

$$G(x,x') = \frac{1}{4\pi}\sum_{n=1}^{\infty}(R_{12})^{n-1}T_{12} \ln\left\{\frac{\left(n^2+(\frac{x-x'}{2d})^2\right)\left(n^2+(\frac{x+x'}{2d})^2\right)}{\left((n-1)^2+(\frac{x-x'}{2d})^2\right)\left((n-1)^2+(\frac{x+x'}{2d})^2\right)}\right\} \tag{63}$$

representing the potentials due to four electric line charges, Fig. 3(c). By some change in notation (63) resembles that obtained earlier by Silvester [1] in the case $\chi = 0$.

When the width of the k'th line charge is w_k, the potential can be written

$$U_k = \left[\sum_{j=1}^{N}\frac{1}{w_k w_j}\int_{w_k}\int_{w_j} G(x,x')\mathcal{M}_1^{-1}dxdx'\right]_{11}$$
$$q_j = \sum_{j=1}^{N} p_{k,j}q_j \tag{64}$$

where the subindex 11 refers to the matrix element. The electric charge per unit length on the jth strip is denoted by q_j. G is the Green's function (63), which can be integrated analytically to yield

$$p_{k,j} = \frac{1}{2\pi}\left\{\left[\sum_{n=1}^{\infty}R_{12}^{n-1}T_{21}\left[\frac{F_{k,j}^{n}}{w_k w_j}-6\right] - I\left[\frac{F_{k,j}^{0}}{w_k w_j}-6\right]\right](\mathcal{M}_1+\mathcal{M}_2)^{-1}\right\}_{11} \tag{65}$$

where

$$F_{k,j}^{n} = F(u_k-l_j,n) - F(u_k+l_j,n) + F(l_k+l_j,n) - F(l_k-l_j,n) + F(l_k-u_j,n) - F(l_k+u_j,n) + F(u_k+u_j,n) - F(u_k-u_j,n)$$
$$F(x,n) = \frac{1}{2}[x^2-(2dn)^2]\ln[(x/2d)^2+n^2] + 4dnx\arctan(x/2dn)$$

Here, u_k, l_k are the upper and lower limits of the kth strip. Setting the potential vector U to unity, we are able to solve for the charge distribution by inversion of the p matrix. Finally, the capacitance per unit length is obtained by

$$C = 2\sum_{k=1}^{N}\sum_{j=1}^{N}(p^{-1})_{k,j} \tag{66}$$

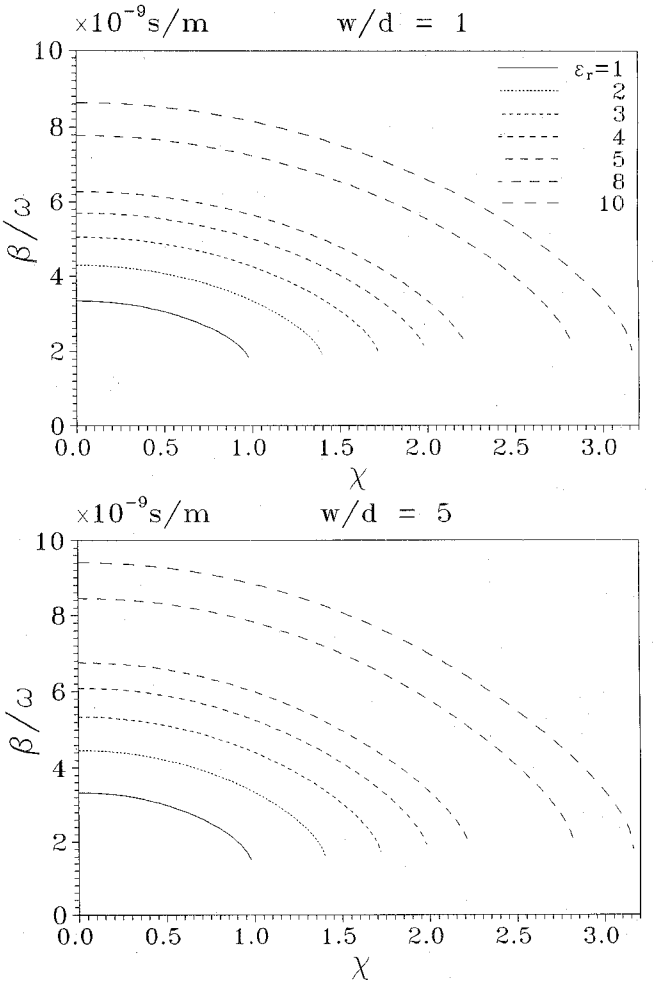

Fig. 4. Normalized propagation constant $B_1 = B$ as a function of χ for different values of E_r of the slab. The permittivity is M_o in all space. Strip width per substrate thickness, w/d, is 1 in the upper and 5 in the lower graph. A subdivision of $N = 30$ has been used throughout these calculations.

Calculations show that the convergence of the series gets slower for increasing χ. It is also seen that in the limit $\chi \to \sqrt{\epsilon_r \mu_r}$, the capacitance approaches zero. This limitation coincide with the condition for positive energy density in the BI medium [4].

The inductance is determined using a similar method as described above for the capacitance. In this case, the integral equation for the magnetic flux ψ_k and the current I becomes

$$\psi_k = \left[\sum_{j=1}^{N}\frac{1}{w_k w_j}\int_{w_k}\int_{w_j} G'(x,x')\mathcal{M}_1 dxdx'\right]_{22} I_j \tag{67}$$

where G' is basically the same Green's function as (63), except for the replacement $\mathcal{M} \leftrightarrow \mathcal{M}^{-1}$. The inductance per unit length is given by the formula

$$L = \frac{1}{2\sum_{k=1}^{N}\sum_{j=1}^{N}(p'^{-1})_{k,j}} \tag{68}$$

When the inductance and capacitance are known, the normalized propagation constant $\beta_1 = \beta/\omega$ can be obtained from (61). Fig. 4 illustrates β_1 as a function of the parameter χ for different values of ϵ_r and for two different strip widths. In Fig. 5, the solid lines illustrate the quasi-static approximation

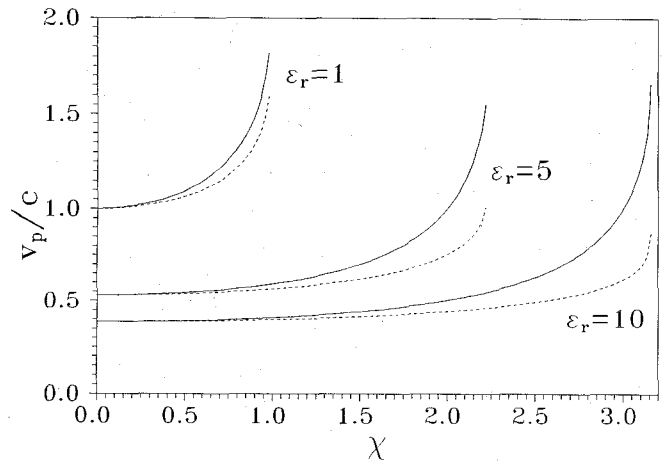

Fig. 5. Normalized phase velocity as a function of χ. Result of quasi-static approximation (solid lines) and static approximation (dashed lines) for different permittivities, when $w/d = 1$.

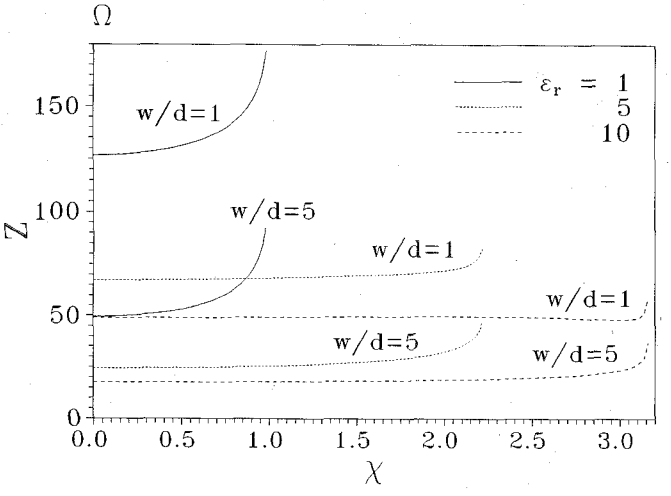

Fig. 6. Characteristic impedance for different strip widths and permittivities.

for phase velocity $v_p = 1/\beta_1$ in the microstrip ($w/d = 1$) as a function of χ. For a comparison, the dashed lines represent the approximation, which only takes into account the effect of capacitance trough the formula $v_p = c\sqrt{C_0/C}$ (i.e., static approximation), where c is the speed of light, and C_0 the capacitance when $\epsilon_r = 1$ and $\chi = 0$. The results for the static and quasi-static approximations are quite similar for small χ values but differ remarkably when χ approaches $\sqrt{\epsilon_r \mu_r}$.

The impedance Z is calculated from (62) for different permittivities and strip widths as a function of χ. Fig. 6 shows that for some values of ϵ_r, the impedance remains almost unchanged although χ varies.

V. Conclusion

The method of partial images has been applied to evaluate different kinds of Green's functions for the microstrip structure with a BI substrate. The magneto-electric coupling property of fields in a BI medium motivated the use of a compact matrix formalism. A special kind of Green's function was developed and applied to the analysis of quasi-static solutions in a microstrip line consisting of an infinitely thin conductor attached on a BI substrate with a PEC backing. Because the quasi-TEM mode is dominating when the wavelength is much greater than the transverse dimensions of the waveguiding structure, the asymptotic series expansion method was applied for the analysis. The transversal zeroth order fields were affected by the three parameters ϵ, μ and χ whereas κ was absent because of the intrinsic frequency dependence of chirality. On the other hand, the chirality was seen to give rise to transversal magnetic field of the first order, in addition to the usual longitudinal fields. To obtain the propagation constant, the capacitance and inductance were calculated numerically for a microstrip structure with different values of strip width per substrate thickness as a function of χ.

References

[1] P. Silvester, "TEM wave properties of microstrip transmission lines," *Proc. IEE*, vol. 115, no. 1, pp. 43–48, Jan. 1968.
[2] I. V. Lindell, "Static image theory for bi-isotropic media with plane parallel interfaces," *Microwave and Optical Tech. Lett.*, vol. 6, no. 4, pp. 226–230, March 1993.
[3] I. V. Lindell, "Static image method for layered isotropic and bi-isotropic cylinders," *Microwave and Optical Tech. Lett.*, vol. 6, no. 6, pp. 383–387, May 1993.
[4] I. V. Lindell, "Quasi-static image theory for the bi-isotropic (nonreciprocal chiral) sphere," *IEEE Trans. Antenn. Propagat.*, vol. 40, no. 2, Feb. 1992.
[5] A. G. O'Neill, "Calculation of the image potential in multiple layered structures," *J. Applied Phys.*, vol. 58, no. 12, pp. 4740–4742, Dec. 1985.
[6] A. F. dos Santos and J. P. Figanier, "The method of series expansion in the frequency domain applied to multidielectric transmission lines," *IEEE Trans. Microwave Theory Tech.*, vol. 23, pp. 753–756, Sept. 1975.
[7] I. V. Lindell, "On the Quasi-TEM modes in inhomogeneous multiconductor transmission lines," *IEEE Trans. Microwave Theory Tech.*, vol. 29, no. 8, pp. 812–817, Aug. 1981.

Päivi Koivisto was born in Seinäjoki, Finland, in 1957. She received the Diploma Engineer degree in technical physics and Licentiate of Technology degree in electrical engineering from the Helsinki University of Technology, Espoo, Finland in 1985 and 1992, respectively. She has been working on fiber- and integrated optics at the Semiconductor Laboratory of the Technical Research Center of Finland from 1984 to 1989. Currently, she is with the Electromagnetics Laboratory of the H.U.T. Her main interests are electromagnetic theory and chiral and bi-isotropic media.

Johan Sten was born in Helsinki, Finland, in 1967. He received the Diploma Engineer degree in electrical engineering from the Helsinki University of Technology, Espoo, Finland in 1992. Currently, he is with the Electromagnetics Laboratory of the H.U.T. His interests are in analytical methods, especially image theories, in electromagnetics.